

Mechanical and Processing Enhancement of a Recycled HDPE/PPR-Based Double-Wall Corrugated Pipe via a POE-g-MAH/CaCO₃/HDPE Polymer Composite

Yutong Wang, Lichang Lu, Yu Hao, Yujie Wu, and Yuanzhe Li*



Cite This: *ACS Omega* 2021, 6, 19705–19716



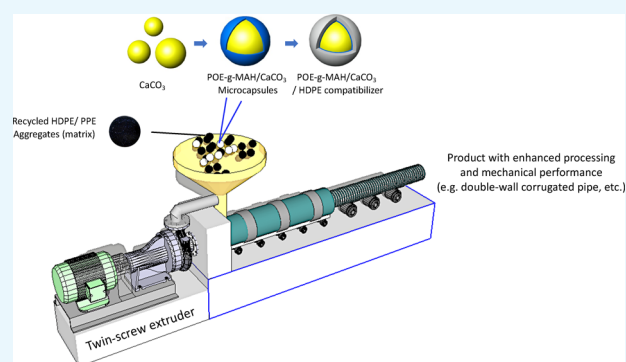
Read Online

ACCESS |

Metrics & More

Article Recommendations

ABSTRACT: With the people's awareness of the "3Rs" in recent years, using recycled high-density polyethylene (HDPE) and random copolymer polypropylene (PPR) as the base materials for piping fabrication has become a mainstream in scholastic path and industrial engineering. In this study, the modified maleic anhydride-grafted polyethylene (POE-g-MAH) compatibilizer was fabricated to increase the interfacial adhesion and dispersion. With the surface modification of calcium carbonate, a POE-g-MAH/CaCO₃/HDPE polymer composite has been prepared. Such modified polymer composites can further reinforce the processing performance and mechanical properties of recycled HDPE and PPR materials. The results indicated that with the introduction of the polymer composite, significant enhancement of the recycled materials in the aspects of processability, tensile strength, flexural performance, and impact force could be obtained, and the POE-g-MAH/CaCO₃/HDPE polymer composite would contribute to the impressive balance between high rigidity and toughness. In addition, the feasibility and mechanical properties of the recycled HDPE-PPR-POE-g-MAH/CaCO₃/HDPE blended system were also studied: with the help of a composite microcapsule, the gap of mechanical capacity between recycled and non-recycled materials was further reduced, and such a blended system was capable of being commercialized in the piping industry.



1. INTRODUCTION

Double-wall corrugated pipes with a cyclic wall structure have been widely used for industrial and daily consumption. Compared with traditional iron, concrete, and even clay pipes, the double wall corrugated pipe has high rigidity, excellent bending performance, high impact and compressive strength, and even other characteristics. Because of their excellent performance and relatively economical cost,¹ double-wall corrugated pipes in Europe and other developed countries have been greatly promoted and applied.²

The raw materials of double-wall corrugated pipes could be generally divided into two categories, which include polyvinyl chloride (PVC) and polyolefin (polyethylene or polypropylene).^{3,4} The PVC piping materials, although compared to polyolefins, have advantages of good stiffness and low-cost over the polyethylene and polypropylene ones, but because of their difficulties in processing, it would become difficult to enlarge the diameter. In addition, the PVC double wall corrugated pipe would have significant impact defects under low temperature.^{3,5} As in the aspect of flexibility, weldability, thickness, aging resistance, and even environmental protection, polyolefin double wall corrugated pipe polyolefin has certain advantages over polyvinyl chloride. Hence, the PVC raw material has been

substituted by polyolefin in the market due to the fierce competition.⁶ Polyolefin double walls mainly contain two types of materials wherein high-density polyethylene (HDPE) and random-copolymer polypropylene (PPR) as the most representative piping materials have their large applications even in some specific areas.⁷ These two piping materials share reliable connection, high impact resistance, chemical resistance, flexibility, water resistance, and other characteristics.⁸

With people's awareness of environmental protection via the "3Rs" (Reduce, Reuse, & Recycle), recycled HDPE and PPR materials have been increasingly developed in the cutting edge.⁹ Not only could it save oil resources by reducing the generation of waste, but also the recycled plastic wastes could be fully utilized. However, as the recycled materials are blended and obtained through extrusion, these samples do not indicate satisfactory mechanical performance compared with

Received: May 5, 2021

Accepted: July 2, 2021

Published: July 20, 2021



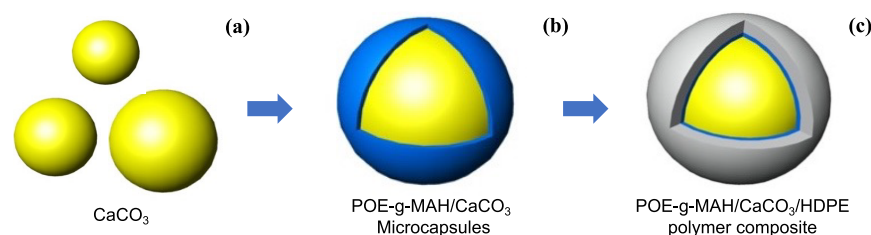


Figure 1. Schematic diagrams of (a) the CaCO_3 microdroplet, (b) POE-g-MAH/ CaCO_3 microcapsule, and (c) POE-g-MAH/ CaCO_3 /HDPE polymer composite.

Table 1. Table of HDPE/PPR Piping Formulations

formulation code name	HDPE/ PPR	POE-g-MAH grafted compatibilizer (test group)	non-POE-g-MAH compatibilizer (control group)	CaO defoamer
non-recycled HDPE/PPR	95			5
5% w POE-g-MAH	90	5		5
15% w POE-g-MAH	80	15		5
25% w POE-g-MAH	70	25		5
35% w POE-g-MAH	60	35		5
45% w POE-g-MAH	50	45		5
55% w POE-g-MAH	40	55		5
5% w/o POE-g-MAH	90		5	5
15% w/o POE-g-MAH	80		15	5
25% w/o POE-g-MAH	70		25	5
35% w/o POE-g-MAH	60		35	5
45% w/o POE-g-MAH	50		45	5
55% w/o POE-g-MAH	40		55	5

non-recycled materials.¹⁰ With the development of inorganic–organic hybrid composites, it is indicated that these inorganic composites are able to continuously improve mechanical and processing properties of the plastic materials. Moreover, attempts to improve mechanical properties for commonly used polyolefins by using ceramic materials, e.g., silicon nitride, glove talc, and silicon carbide, have been carried out in recent technical studies.^{11,12} The addition of inorganic composite-reinforced polyolefins, such as high-density polyethylene (HDPE) and random copolymer polypropylene (PPR), has also been reviewed by various authors.^{13–15} However, the major problem in these recycled composites is still the interfacial adhesion between the inorganic filler and the polyolefin matrix as well as their dispersion. Deka et al.¹⁶ introduced an epoxy functionalized hybrid compatibilizer to address the interfacial bonding; Deepthi et al.¹⁷ used surfaces treated with cenospheres and a functionalized high-density polyethylene (HDPE) to improve the compatibility between the blend components.

In this study, the modified POE-g-MAH/ CaCO_3 /HDPE polymer composite has been fabricated for the improved compatibility of the interfacial adhesion between the HDPE/PPR matrix and inorganic calcium carbonate. After it was further blended with HDPE and PPR, the processing rheology and mechanical studies of such blended systems have been conducted. These results include the enhancement of processing and mechanical properties of these recycled materials and even offer the formulation optimization of the mass percentage of the compatibilizer in practical applications.

2. MATERIALS AND METHODS

2.1. Materials. Recycled HDPE aggregates (Brand M) and recycled PPR aggregates (Brand X) were purchased from Jingcheng Plastic Co., Ltd. (Chengdu, China) and Maoguang

Plastic Co., Ltd. (Chengdu, China), respectively. The other groups of non-recycled HDPE aggregates and non-recycled PPR aggregates were also selected for analogical experiments and benchmarks from the same companies. Ethylene-alpha-octene copolymer, maleic anhydride (MAH), and a peroxide-type initiator¹⁸ were obtained from Dow Chemical Pacific Ltd. (Selangor, Malaysia) for the fabrication of the POE-g-MAH (maleic anhydride-grafted polyethylene) compatibilizer. Antioxidant 1010 (pentaerythritol tetrakis-3-(3,5-di-*tert*-butyl-4-hydroxyphenyl) propionate), calcium oxide (CaO) defoamers,¹⁶ calcium carbonate (CaCO_3), and styrene were obtained from Sigma-Aldrich (Shanghai, China).

2.2. Preparation of the Modified POE-g-MAH Compatibilizer. The maleic anhydride (MAH)-grafted polyolefin thermoplastic elastomer (POE) was prepared by mixing an ethylene-alpha-octene copolymer, maleic anhydride (MAH), a peroxide-type initiator, and phosphite. The ethylene-alpha-octene copolymer was a vinyl elastomer made from ethylene and an alpha-octene copolymer. It is a new type of polyolefin thermoplastic elastomer (POE) developed by the Dow Chemical Company in the US using metallocene as the catalyst. After simple mixing, all the raw materials, calcium carbonate, and Antioxidant 1010, with a ratio of 98:1:1 by mass, were put into an extruder or compactor for a melt grafting reaction to obtain the said maleic anhydride-grafted ethylene-alpha-octene copolymer following ref 18.

2.3. Surface Modification of Calcium Carbonate. Figure 1 presents the schematic diagrams illustrating the formation of the POE-g-MAH/ CaCO_3 /HDPE polymer composite. CaCO_3 microdroplets (Figure 1a) were dispersed uniformly in the polymer composite with the help of calcium oxides and Antioxidant 1010. After adding POE-g-MAH and stirring, POE-g-MAH/ CaCO_3 was formed and stabilized with the presence of a microcapsule structure bigger than the

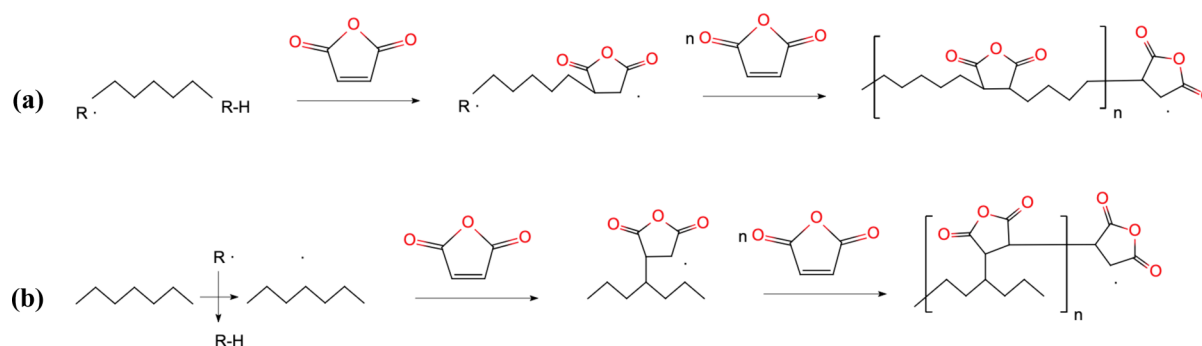


Figure 2. Formation mechanism of POE-g-MAH: (a) backbone polymerization and (b) side grafted polymerization.

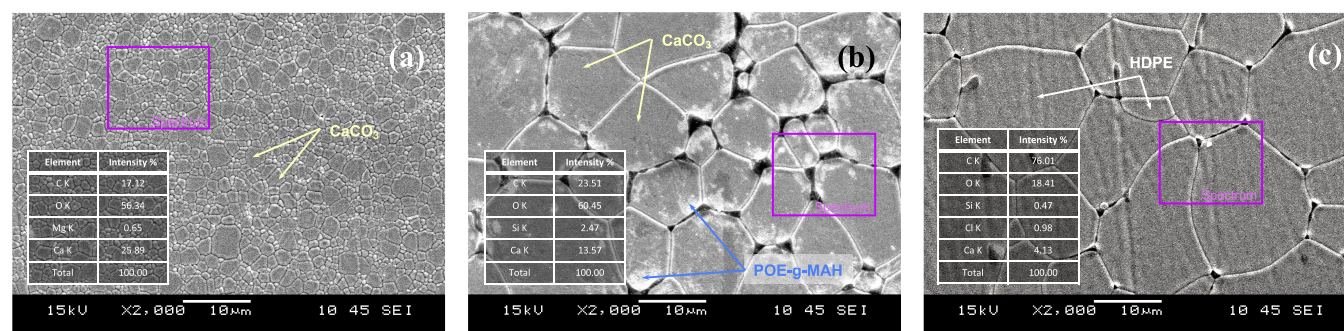


Figure 3. SEM graphs and EDX mappings of (a) the CaCO_3 microdroplet, (b) POE-g-MAH/ CaCO_3 microcapsule, and (c) POE-g-MAH/ CaCO_3 /HDPE polymer composite.

original CaCO_3 , as shown in Figure 1b,c. Such a polymer composite was filling-synthesized by the extrusion of POE-g-MAH (modified maleic anhydride-grafted elastomer): CaCO_3 :HDPE at 1:16:3 by mass. Continuous stirring and heating were carried out for 2.5 h at 125 °C. The grafted product was cooled and precipitated in methanol and filtered. The product obtained was then washed several times with methanol, rinsed with acetone for cleaning the composite surface, and dried for further usage. Meanwhile, the control polymer-composite group with no POE-g-MAH compatibilizer was fabricated by CaCO_3 :HDPE only at 4:1 in the same process.

2.4. Blending Preparation of the Newly Fabricated Recycled Pipe Materials. The newly fabricated recycled pipe materials were added into a PS40E5ASE injection molding machine (NISSEI, Shenzhen, China) with the following processing parameters: temperature at the front end of 220 °C, middle temperature of 220 °C, and temperature at the rear end of 180 °C; extrusion rate of 16%; injection time of 12.0 s; molding time remaining at 30.0 s; and cooling time of 2.0 s.⁸ The piping formulations are indicated in Table 1. CaO at 5.0 wt % was selected as the default defoamer within formulations.¹⁸

2.5. Composition and Morphology Characterization. The morphology was characterized using a scanning electron microscope (SEM) (Hitachi S-4700, California, US) that was attached to a Bruker AXS Quantax 4010 energy-dispersive X-ray spectrometer (EDX, Karlsruhe, Germany).⁹ FTIR spectra were obtained at room temperature on a Nicolet - 6700 spectrophotometer (Thermo Electron Corporation, Waltham, US) between 4000 and 600 cm^{-1} with a resolution of 4 cm^{-1} .¹⁰

2.6. Processing Rheology. The processing rheology, including the melt flow rate (MFR), was performed on the

capillary rheometer CFT-500D (SHIMADZU/SSL, Shanghai, China). 1.0 g of the blended samples was selected, the experimental temperature was at 200 °C, load weight was at 9.5 kg, and the capillary specifications were $\Phi 1.0 \times 10.0$ mm.¹¹

2.7. Mechanical Properties of the Blends. The tensile and flexural properties of the nanocomposites were measured using an AGS-J (SHIMADZU/SSL, Shanghai, China). The tensile and flexural tests were performed as per ASTM:D638 and ASTM:D790-10 methods, respectively.^{12,13} The impact test was performed using an XQZ-1 (Minsks, Xi'an, China) first to hit the samples with 2.0 mm deep type A pendulum followed by an XJU-5.5 Izod impact tester (Tuobo, Suzhou, China) on the notch test specimens with the pendulum at 2.75 J.^{14,15} A minimum of five specimens was tested for each variation in composition of the blend, and results were averaged.

3. RESULTS AND DISCUSSION

3.1. Formation Mechanism of the POE-g-MAH Compatibilizer. Figure 2 indicates the potential reactions that occurred in the formation of the maleic anhydride (MAH)-grafted polyolefin thermoplastic elastomer (POE). The polyolefin elastomer contained between 9.5 and 28.0% by weight alpha-octene. The polyolefin elastomer had a melt index (MFR, ASTM D-123B) of 1–30. The polyolefin elastomer had a narrow relative molecular weight distribution and a narrow comonomer distribution.^{6,11} The polymerization, wherein $n = 5000$ to 30,000, might happen in both the backbone (Figure 2a) and side chain (Figure 2b) with the following repeating structural units. The high weight percentage of side grafted MAH could lead to more spatial structures for the packaging of other organic and inorganic particles. According to Figure 2, the preparation started with creating a POE-g-MAH emulsion with spatial structures.

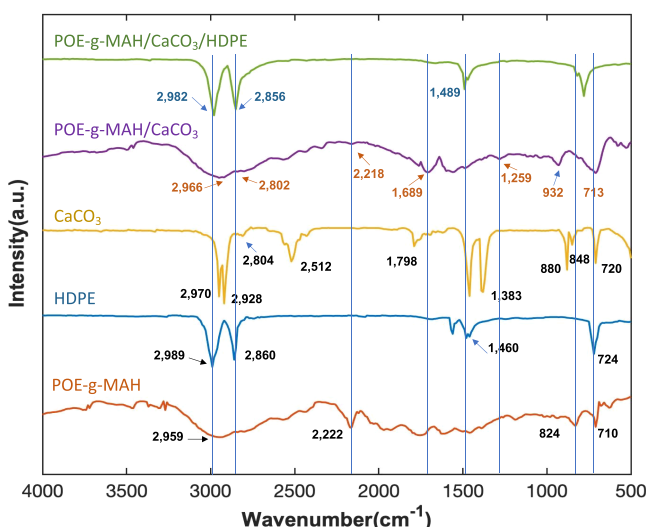


Figure 4. FTIR spectra of the compatibilizer component POE-g-MAH, pure HDPE, the CaCO_3 microdroplet, the POE-g-MAH/ CaCO_3 microcapsule, and the POE-g-MAH/ CaCO_3 /HDPE polymer composite.

3.2. SEM Characterization of the POE-g-MAH/ CaCO_3 /HDPE Polymer Composite. The surface modification of calcium carbonate was obtained by covering the POE-g-MAH/ CaCO_3 microcapsules with an HDPE shell and a POE-g-MAH/ CaCO_3 /HDPE polymer composite emerged. Through the high-energy beam of electrons under SEM observation, the corresponding structures of the CaCO_3 microdroplet, POE-g-MAH/ CaCO_3 microcapsule, and POE-g-MAH/ CaCO_3 with an HDPE shell are demonstrated in Figure 3. The POE-g-MAH thin film on the CaCO_3 microdroplet contained a small CaCO_3 microdroplet by forming a new grain boundary, as shown in Figure 3a. The thin HDPE shell effectively stabilized and prevented the coalescence of POE-g-MAH/ CaCO_3 microcapsules and served as the hard template for the newly fabricated compatibilizer (Figure 3c). Also, the appearance of the polymer composite was as white in color as its CaCO_3 base. Through EDX mapping in Figure 3, the intensities for the different elements within the spectra are indicated as well. The intensity change, comparing among Figure 3a–c of the calcium element, would provide sufficient evidence of the inorganic calcium carbonate in the POE-g-MAH/ CaCO_3 microcapsule.

There might be a lot of calcium carbonate in there all stuck together, but with proper mixing with HDPE, a thin shell was formed from the reaction between POE-g-MAH and HDPE due to the high reactivity of POE-g-MAH.

3.3. FTIR Characterization of the POE-g-MAH/ CaCO_3 /HDPE Polymer Composite. To confirm that the POE-g-MAH/ CaCO_3 /HDPE polymer composite has been successfully prepared, the FTIR spectra of the different stages of POE-g-MAH/ CaCO_3 /HDPE polymer composite were obtained, as shown in Figure 4. To prove that POE-g-MAH was grafted on CaCO_3 , pure HDPE used for polymer composite preparation, POE-g-MAH (both as a control group), and the POE-g-MAH/ CaCO_3 microcapsule was extracted with the ethanol solvent. Then, the residues were characterized by FTIR. According to the functional groups as confirmed by the literature,^{16–18} the POE-g-MAH/ CaCO_3 microcapsule exhibited the absorption peaks of POE-g-MAH at 2966, 2802, 2218, 1689, 1259, 932, and 713 cm^{-1} marked in brown,¹⁶ but its spectra might have been affected and still retained similar absorption peaks to CaCO_3 at 2804, 1798, 848, and 720 cm^{-1} .¹⁷ As for the spectra for the POE-g-MAH/ CaCO_3 microcapsule, there was some migration that happened compared with CaCO_3 , but after comparing it with the product after solvent extraction, it was not obvious to observe the mitigation of peaks among different composites. Also, this might be caused by the complex spatial structure in between POE-g-MAH and CaCO_3 .

After the POE-g-MAH/ CaCO_3 /HDPE polymer composite was formed, the FTIR spectra only displayed most of the characteristic peaks of HDPE at 2982, 2856, and 1489 cm^{-1} as illustrated in dark blue.^{17,18} The peaks of individual CaCO_3 or POE-g-MAH were merged and became smooth, which might indicate the coverage and distribution of HDPE and POE-g-MAH/ CaCO_3 microcapsules and the immobilization of CaCO_3 in the polymer composite. Transmission electron microscopy (TEM) images for all the samples were also obtained for their interfacial characterizations. However, as the transparency for the samples was very low, the distribution of CaCO_3 microdroplets within the composite and microcapsule could be barely seen in Figure 5a–c with different magnifications. The interface between the CaCO_3 microdroplet and POE-g-MAH/ CaCO_3 microcapsule was marked, and the surrounding irregular structure attached with the microcapsule was believed to be the HDPE matrix. Such

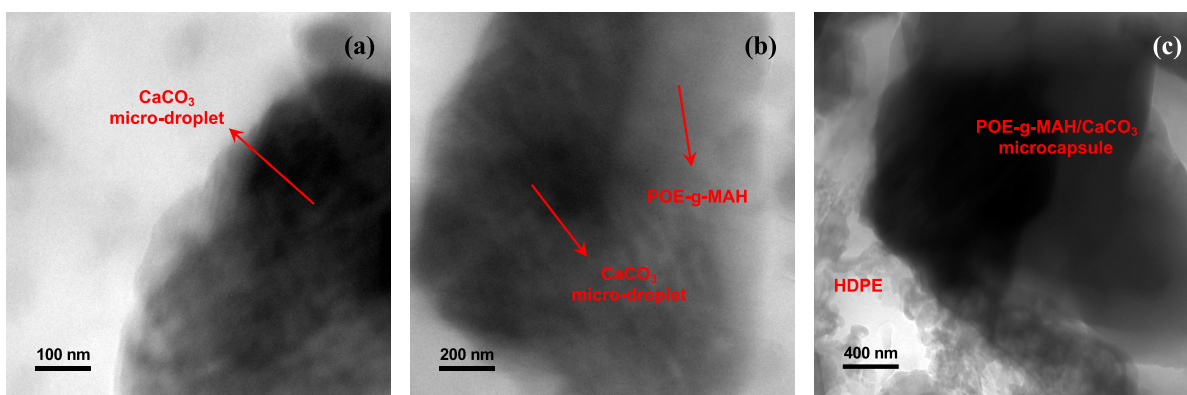


Figure 5. TEM images of the POE-g-MAH/ CaCO_3 /HDPE polymer composite at different magnifications: (a) structures of the CaCO_3 microdroplet, (b) interface between POE-g-MAH and CaCO_3 within the POE-g-MAH/ CaCO_3 microcapsule, and (c) interface within the polymer composites.

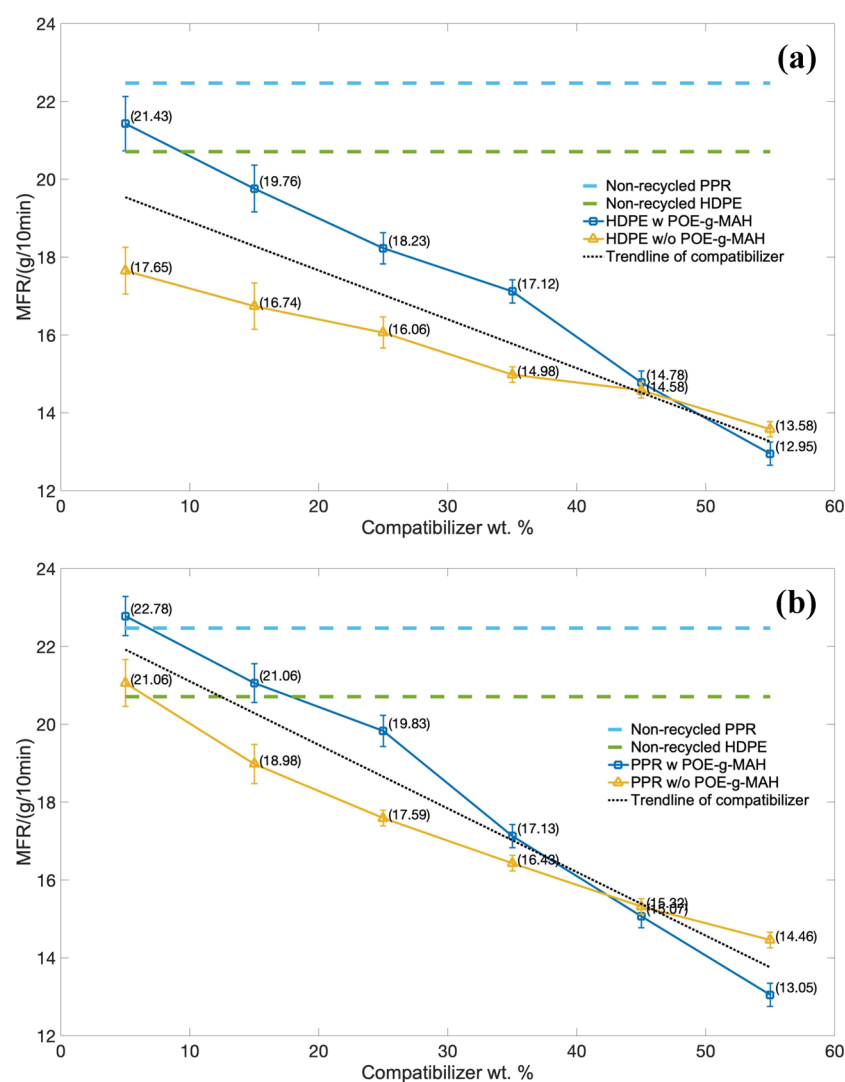


Figure 6. Melt flow rate (MFR) over the mass of the compatibilizer: (a) HDPE series and (b) PPR series.

Table 2. Shear Rate, Viscosity, and Flow Rate of the HDPE Series

formulation code name	flow rate $\times 10^{-2}/(\text{cm}^3/\text{s})$	viscosity $\times 10^2/(\text{Pa}\cdot\text{s})$	shear rate $\times 10^2 / \text{s}^{-1}$
non-recycled HDPE	3.49 ± 0.22	6.97 ± 0.15	3.53 ± 0.47
5% w POE-g-MAH	3.23 ± 0.12	7.26 ± 0.73	3.28 ± 0.13
15% w POE-g-MAH	2.85 ± 0.51	8.14 ± 0.19	2.93 ± 0.81
25% w POE-g-MAH	2.67 ± 0.09	8.99 ± 0.14	2.72 ± 0.17
35% w POE-g-MAH	2.49 ± 0.27	9.63 ± 0.99	2.54 ± 0.62
45% w POE-g-MAH	2.43 ± 0.15	9.91 ± 0.12	2.47 ± 0.59
55% w POE-g-MAH	2.26 ± 0.33	10.64 ± 0.58	2.31 ± 0.28
5% w/o POE-g-MAH	3.04 ± 0.13	7.52 ± 0.34	3.15 ± 0.29
15% w/o POE-g-MAH	2.79 ± 0.27	8.24 ± 0.22	2.91 ± 0.28
25% w/o POE-g-MAH	2.58 ± 0.11	8.74 ± 0.55	2.74 ± 0.19
35% w/o POE-g-MAH	2.40 ± 0.72	9.43 ± 0.77	2.53 ± 0.82
45% w/o POE-g-MAH	2.29 ± 0.48	9.87 ± 0.92	2.42 ± 0.29
55% w/o POE-g-MAH	2.14 ± 0.54	9.98 ± 0.79	2.28 ± 0.45

interfacial adhesion could also be concluded from the previous SEM characterization section.^{19,20}

3.4. Processing Performance Analysis of the Newly Fabricated Recycled Pipe Materials. The processing rheology, which represented the processability of the melt flow rate (MFR), was performed under the same applied stress at 2.45×10^5 Pa. The HDPE series piping material with the

MFR over the mass percentage of the compatibilizer is indicated in Figure 6a, and the PPR-based series is indicated in Figure 6b.

For the HDPE piping series, the MFR of the composites decreased with the increment of two compatibilizers as demonstrated in the trend line. The same decreasing tendency also happened in the PPR piping series, which can be

Table 3. Shear Rate, Viscosity, and Flow Rate of the PPR Series

formulation code name	flow rate $\times 10^{-2}$ / (cm^3/s)	viscosity $\times 10^2$ / ($\text{Pa}\cdot\text{s}$)	shear rate $\times 10^2$ / s^{-1}
non-recycled PPR	3.74 ± 0.27	6.426 ± 0.29	3.82 ± 1.26
5% w POE-g-MAH	3.57 ± 0.22	6.795 ± 0.84	3.73 ± 0.57
15% w POE-g-MAH	3.48 ± 0.23	7.231 ± 1.22	3.52 ± 0.63
25% w POE-g-MAH	3.21 ± 1.17	7.945 ± 1.27	2.98 ± 0.91
35% w POE-g-MAH	2.98 ± 0.36	8.646 ± 0.93	2.94 ± 0.52
45% w POE-g-MAH	2.67 ± 0.29	9.735 ± 0.56	2.64 ± 0.43
55% w POE-g-MAH	2.43 ± 0.43	10.523 ± 0.43	2.47 ± 0.27
5% w/o POE-g-MAH	3.58 ± 1.19	6.673 ± 0.53	3.71 ± 0.41
15% w/o POE-g-MAH	3.47 ± 0.18	6.842 ± 0.41	3.50 ± 1.23
25% w/o POE-g-MAH	3.31 ± 0.27	7.281 ± 0.98	3.37 ± 0.51
35% w/o POE-g-MAH	2.85 ± 0.46	8.430 ± 1.15	2.91 ± 0.48
45% w/o POE-g-MAH	2.52 ± 1.12	9.582 ± 0.42	2.59 ± 0.37
55% w/o POE-g-MAH	2.37 ± 0.31	9.801 ± 1.19	2.32 ± 1.02

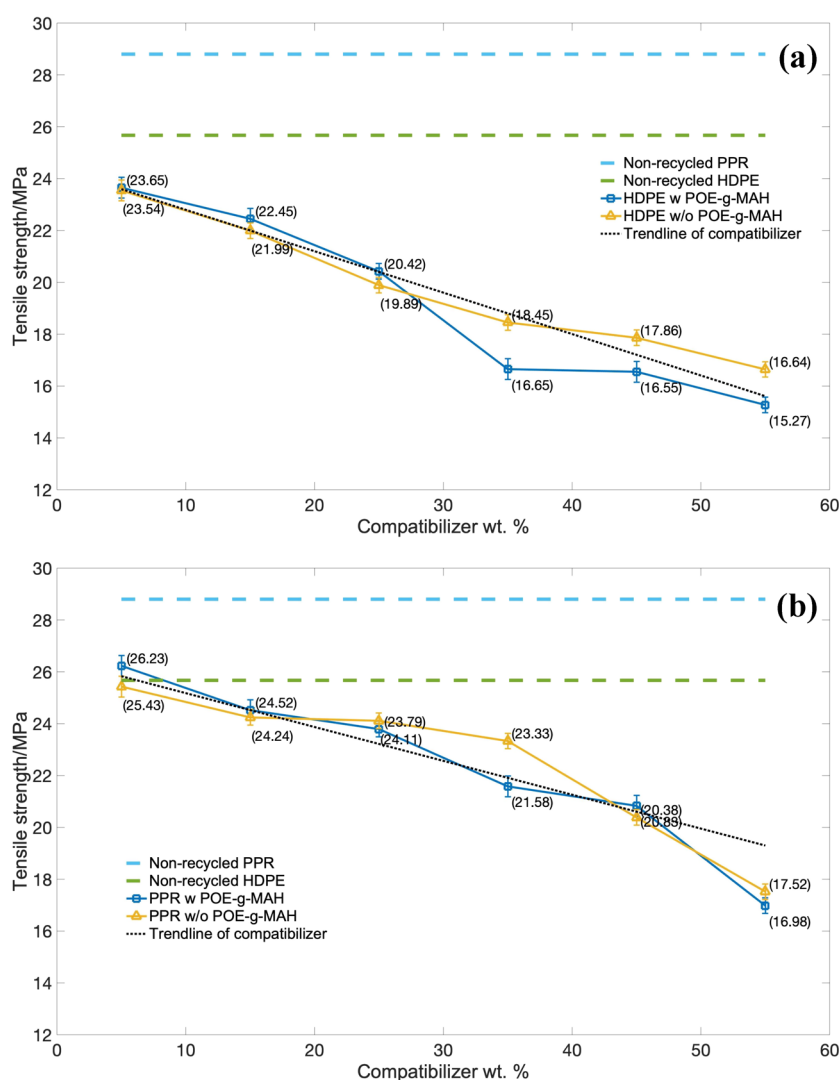


Figure 7. Tensile strength (TS) over the mass of the compatibilizer: (a) HDPE series and (b) PPR series.

summarized as follows: the more the compatibilizer used, the smaller the melt flow rate becomes. The reason could be due to the large possibility of the CaCO_3 filler particles gathering together in the composite blending system. As most of the fluidity within the composite changed to aggregating state, the MFR reduced. However, with the help of the grafted POE-g-MAH, the decrement of the flowability and the MFR would

become slower than the groups without POE-g-MAH. Even at a lower weight percentage of compatibilizer, the MFR performance would be better than those of pure HDPE and PPR. It should be caused by the core-shell structure composed of individual CaCO_3 and POE-g-MAH, and it could increase the dispersion and the faster thermal response during the process.

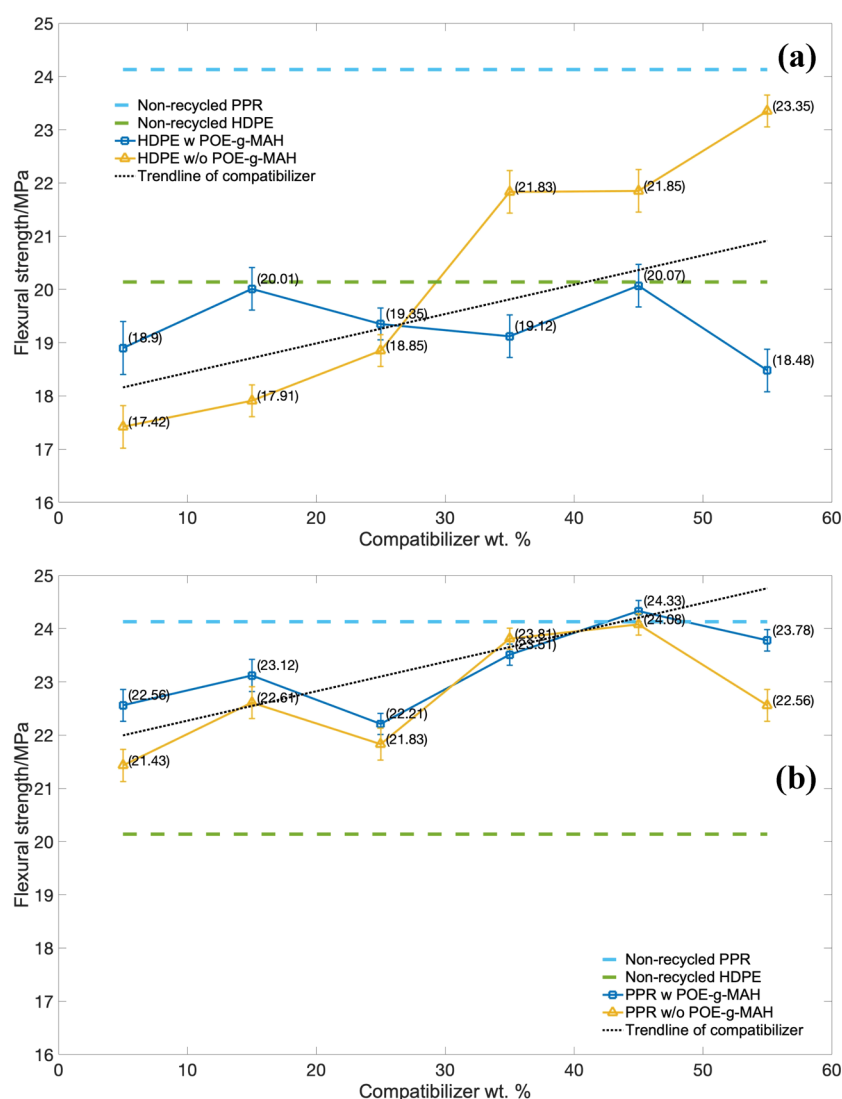


Figure 8. Flexural strength (TS) over mass of compatibilizer: (a) HDPE series and (b) PPR series.

Also, the values of shear rate, viscosity, and flow rate with the samples in the capillary rheometer test were also obtained, as shown in Tables 2 and 3. Although the MFR and processability might be continuously decreasing for both HDPE and PPR with and without POE-g-MAH, still with little amount of POE-g-MAH, the processing performance became higher than those of the non-recycled materials compared with the imaginary lines. To conclude, the more that the mass of the compatibilizer was increased, the worse the flowability and processability we would end up with.

3.5. Mechanical Properties of the Newly Fabricated Recycled Pipe Materials. **3.5.1. Tensile Strength.** The results of tensile strength (TS) of the HDPE series piping material with the strain over the stress are indicated in Figure 7a, and the PPR-based series is indicated in Figure 7b. As indicated in the figure, both the tensile strengths of the HDPE and PPR series decreased with the increment of the compatibilizer. Also, with the greater amount of CaCO_3 particles, worse compatibility was demonstrated between the original polyolefins and these compatibilizers as well as the poorer dispersibility of particles in the base particle. As the samples were subjected to tensile force, the CaCO_3 particles easily fell off the interface, gaps would become larger, and the

tensile strength decreased. It was also indicated that the use of the graft POE-g-MAH compatibilizer in both polyolefin series led to similar tensile strength than without the use of POE-g-MAH.

3.5.2. Flexural Properties. The results of flexural strength of the HDPE series piping material over the stress are indicated in Figure 8a, and the PPR based-series is indicated in Figure 8b. The same values of blue and green imaginary lines are also provided in Figure 8a,b, which could be referred to from there to see the variation between the POE-g-MAH compatibilizer and the flexural strength. For both HDPE and PPR series, the introduction of POE-g-MAH into the two series composites would increase the flexural strength from the demonstration of the trend line. This was due to the addition of the composite particles and its core-shell structure blocking the movement of the molecular chain, and the flexural strength of the composites could be enhanced. Compared with the PPR series, there was a remarkable improvement for the HDPE series without POE-g-MAH with the increment as high as 5.93 MPa, from 17.42 to 23.35 MPa, which indicated the great enhancement of these CaCO_3 -based compatibilizers in the recycled high-density polythene. In order to exhibit the significance of POE-g-MAH within the PPR series, the region

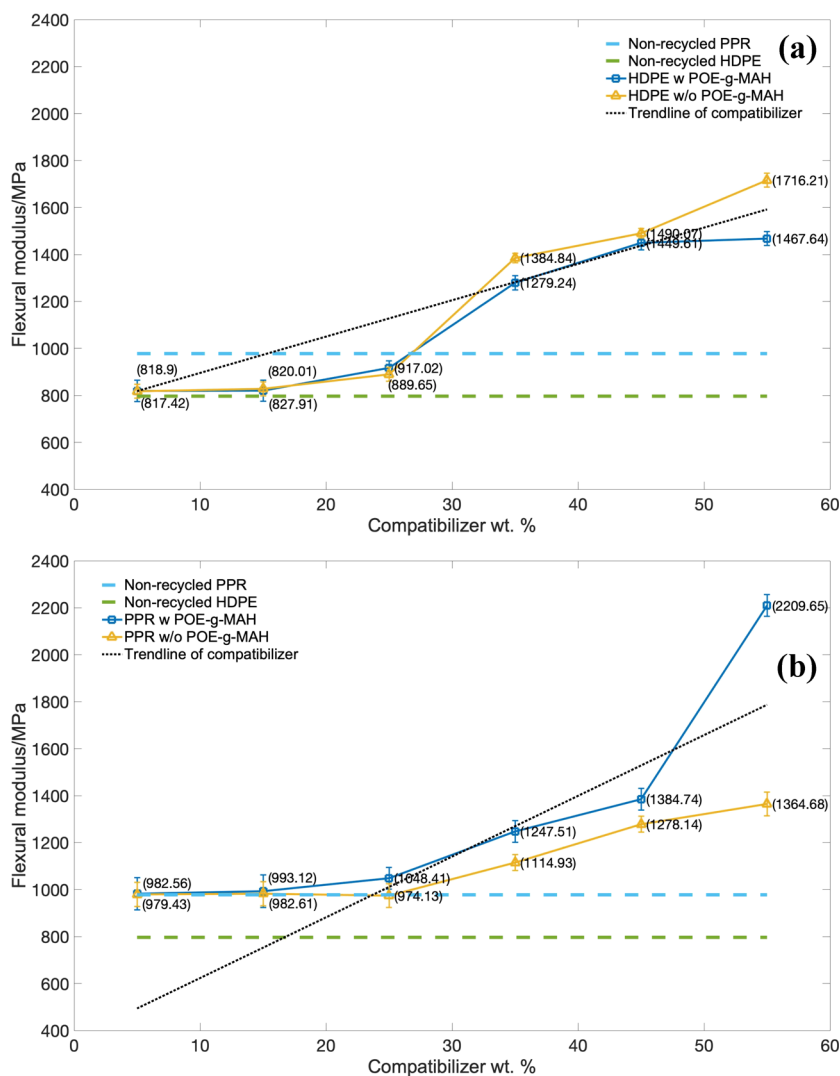


Figure 9. Flexural modulus (FM) over the mass of the compatibilizer: (a) HDPE series and (b) PPR series.

between blue and green imaginary lines was zoomed up. For the PPR series, although there was a slight increase from 22.6 MPa with 5% and 23.8 MPa with 55%, still these small trends would matter in the selection of HDPE-PPR-POE-g-MAH/CaCO₃-blended system, which would be further discussed in following section.

Furthermore, the usage of the POE-g-MAH/CaCO₃/HDPE polymer composite indicated the significant increase compared with the ones without the polymer composite in both HDPE and PPR series. The composite did not have much of an affect for the flexural strength at all mass ratios. Moreover, a slight decrement would even occur as the mass ratio gradually increased from 15 to 35%. Also, the decreasing intervals of the HDPE series were higher than those of the PPR series reaching 1.5 MPa. As shown in Figure 8a,b, as the weight percentage of the POE-g-MAH/CaCO₃/HDPE polymer composite went to 35 and 25%, there was minimum flexural strength for the HDPE and PPR series, respectively. This is because the POE-g-MAH/CaCO₃/HDPE polymer composite was well dispersed in the recycled HDPE and PPR-blended system, which was able to enhance the toughness of the composites rather than the flexural strength.

The results of flexural modulus (FM) of the DPE series piping material over the stress are indicated in Figure 9a, and

the PPR series is indicated in Figure 9b. For the trend lines of both HDPE and PPR series, the increment of these two compatibilizers would significantly increase the flexural modulus. This was due to the modulus of the CaCO₃ particles would be ten to hundred times of the pure polyolefins. In addition, the increment in the HDPE series was higher than those corresponded PPR groups, which indicated the better dispersion of CaCO₃-based compatibilizers in HDPE-blended systems.

Moreover, the flexural modulus of the HDPE series without the POE-g-MAH elastomer was superior to those of the groups with the POE-g-MAH elastomer. This was because of the POE-g-MAH elastomer and its microcapsule structure would enhance the toughness rather than flexural modulus as pre-discussed in flexural strength. While in the PPR series, the increment for the group with POE-g-MAH/CaCO₃ microcapsules indicated better flexural modulus performance, and it was definitely caused by the better dispersion without the help of POE-g-MAH. Also, the whole series of PPR did not increase as much from 5 to 55% of mass as those HDPE series.

In general, with the consideration for both flexural strength and flexural modulus, the addition of compatibilizers had an enhancing effect on the bending performance for both HDPE and PPR series. For the HDPE series, though the introduction

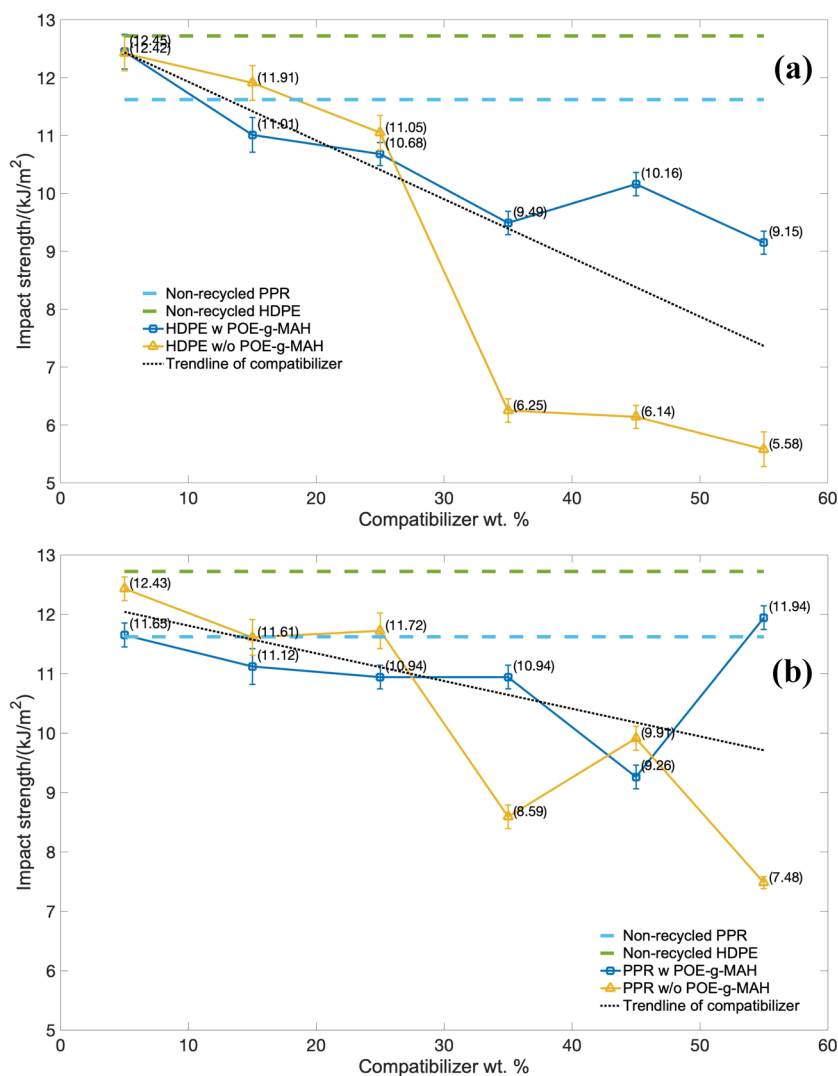


Figure 10. Impact strength over the mass of the compatibilizer: (a) HDPE series and (b) PPR series.

of the POE-g-MAH elastomer would slightly increase the flexural performance, it would obtain a balance between high flexural properties and high toughness. While for the PPR series, the POE-g-MAH elastomer would significantly increase the flexural performance only, it would only donate the effect of CaCO_3 particles in the recycled PPR.

3.5.3. Impact Performance. The results of impact strength (IS) of the HDPE series piping material over the weight percentage of the compatibilizer are indicated in Figure 10a, and the PPR-based series is indicated in Figure 10b. As for both of these two series, the introduction of CaCO_3 particles could substantially increase the notched impact strength and the rigidity of the composites, which was presented in the trend lines for all these groups. Conversely, the toughness for the composites would be reduced. Generally, the more particles there are inside these two blended systems, the poorer the toughness and the worse the impact properties the composite would be; and the PPR series indicated better impact performance than the corresponding HDPE series.

The results also indicated that the use of the POE-g-MAH compatibilizer in both polyolefin series had higher impact strength than the one without the POE-g-MAH compatibilizer, especially at its high mass regions. Although the weight percentage of POE-g-MAH compatibilizer continuously rose to

45%, there was still a certain impact strength increased mutation more in those HDPE series than PPR. The same tendency happened for the PPR series at the mass of 55%, which was even higher than the non-recycled PPR. All these results demonstrated that the impact properties, owing to the POE-g-MAH-grafted compatibilizer, would increase the impact strength and might even obtain a balance with the toughness as well. In sum, the introduction of any compatibilizers into the recycled HDPE and PPR blended system would slightly decrease the impact strength, wherein the formulation groups with the POE-g-MAH compatibilizer would drop less, because of the toughening effect from the POE-g-MAH.

3.6. Formulation Analysis of the Tertiary HDPE/PPR and POE-g-MAH/ CaCO_3 /HDPE-Blended System. For visual representation of the how the mass of this polymer composite in Figure 11 would affect individual factors, including melt flow rate (MFR), tensile strength (TS), flexural strength (FS), flexural modulus (FM), and impact strength (IS), and even for the overall performance, a formulation analysis graph using a normalized unit (p.u.) was obtained. The design of such a figure was to deploy all the experimental results obtained above into one figure for each series (PPR or HDPE) into a normalized unit. Hence, the closer the performance was to 1, the better the performance it referred

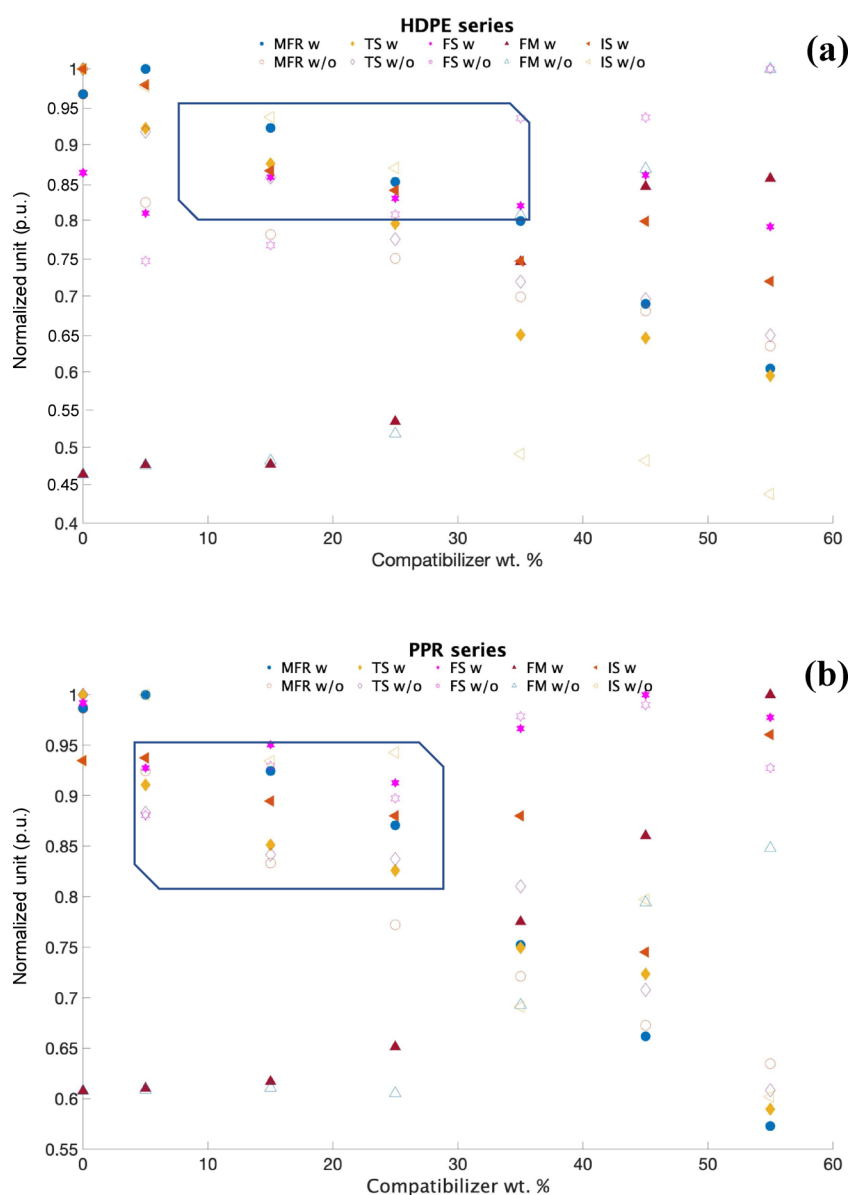


Figure 11. Formulation analysis by using the normalized unit over the mass of the compatibilizer: (a) HDPE series and (b) PPR series.

Table 4. Mechanical Properties of the Recycled HDPE-PPR-POE-g-MAH/CaCO₃ Blended System

HDPE:PPR:POE-g-MAH/CaCO ₃ /HDPE	maximum bending stress (MPa)	flexural modulus (MPa)	impact strength (J)	maximum tensile stress (MPa)
1:1:1	19.05 ± 4.11	553.97 ± 10.82	0.60 ± 0.03	16.08 ± 4.52
2:3:1	24.42 ± 3.72	1033.14 ± 20.72	0.40 ± 0.02	16.85 ± 5.13
3:3:2	22.61 ± 4.51	1342.38 ± 22.13	0.34 ± 0.09	18.14 ± 3.78
3:2:1	21.78 ± 4.09	1256.43 ± 21.42	0.38 ± 0.07	17.89 ± 4.85
2:2:1	21.55 ± 4.69	978.96 ± 19.51	0.36 ± 0.09	24.44 ± 6.95

Table 5. Mechanical Properties of Non-recycled HDPE-PPR-POE-g-MAH/CaCO₃ Blended System

HDPE:PPR:POE-g-MAH/CaCO ₃ /HDPE	maximum bending stress (MPa)	flexural modulus (MPa)	impact strength (J)	maximum tensile stress (MPa)
1:1:1	21.90 ± 3.35	1010.44 ± 20.07	0.38 ± 0.88	15.31 ± 3.90
2:3:1	22.91 ± 4.14	1011.31 ± 19.93	0.38 ± 0.41	17.55 ± 5.10
3:3:2	20.48 ± 3.72	1258.31 ± 22.01	0.46 ± 0.37	12.24 ± 3.40
3:2:1	20.42 ± 3.93	815.69 ± 18.10	0.37 ± 0.21	19.95 ± 4.60
2:2:1	20.79 ± 3.82	902.61 ± 20.12	0.37 ± 0.16	22.35 ± 4.09

to. Also, this method was commonly used in statistics and might help in the selection for the overall best formulation.

Also, the formulation groups with (w) and without (w/o) polymer composites are also included in the figures. It was not

difficult to find that (i) as the overall normalized unit of PPR series was higher: the PPR series recycled materials had its lowest normalized score at 0.57, indicating the slightly better performance of the recycled HDPE series with the lowest score at 0.45; (ii) the processing performance and mechanical properties was very sensitive to the mass of polymer composites. Considering the variations of these five factors and even the opposite tendency among these factors, a region of normalized unit within the range of 0.80–0.95 and concentrated distribution was encircled in Figure 11a,b as well. Moreover, this shaded area should be where the exact optimal formulation group falls in; (iii) due to the different component of the recycled materials, what these results might offer was just the range of the weight percentage of the polymer composite; (iv) for the recycled HDPE series, the optimized formula region of the polymer–composite mass would be in the range between 8 and 35%, while for the PPR series, the optimized region of polymer–composite mass would be at 5 to 25%. In addition, these results might help in the formulation design of HDPE-PPR-POE-g-MAH/CaCO₃ blended systems in the following section.

3.7. Performance Analysis of the HDPE-PPR-POE-g-MAH/CaCO₃/HDPE Blended System. According to the results and discussion of mechanical performance, recycled high-density polypropylene (HDPE) was characterized with good mechanical properties and enhanced rigidity. At the same time, due to the high tensile strength of recycled random copolymer polypropylene (PPR) and good bending resistance, these results did provide important reference and possibility for the fabrication of a POE-g-MAH/CaCO₃/HDPE blended system. Moreover, mixing with a twin screw extruder would contribute to higher impact strength as compared to direct injection.²⁸

Trials of the HDPE-PPR-POE-g-MAH/CaCO₃/HDPE blended system were also performed. Several optimized formulations were selected and their tensile, flexural, and impact properties were studied, indicated in Tables 4 and 5. Table 4 shows that the mechanical properties of the recycled materials would increase and then decrease with the mass increment of the POE-g-MAH/CaCO₃/HDPE polymer composite. The best mechanical performance formulation groups would be the ones with a mass ratio of 3:2:1 for HDPE:PPR:POE-g-MAH/CaCO₃/HDPE, which included a higher HDPE mass (16.7%) than PPR or POE-g-MAH/CaCO₃/HDPE. This was because the structure of polypropylene is easier to be oxidized and degraded under ultraviolet light and heat due to PPR having a methyl side chain before being recycled.

It could also be observed that the non-recycled material for such blended systems would have the best mechanical performance for the formulation group with a HDPE:PPR:POE-g-MAH/CaCO₃/HDPE mass ratio of 2:3:1, which contained less HDPE than the recycled groups. Furthermore, the gap between recycled and non-recycled materials, in Table 5, was further reduced, and such a blended system did prove the mechanical capacity of recycled materials might be better than that of the non-recycled ones. This trial study could also lead to significant commercial development.

4. CONCLUSIONS

This experiment used a modified POE-g-MAH/CaCO₃/HDPE polymer composite to enhance the recycled high-density polyethylene and polypropylene for better preparation

of a double-wall corrugated pipe. The fabrication mechanism of POE-g-MAH/CaCO₃ microcapsules and the processing performance and mechanical properties for different piping formulations were investigated.

The POE-g-MAH/CaCO₃/HDPE polymer composite was able to reinforce the recycled HDPE and PPR by obtaining significant improvement in processability, flexural performance, impact force, and even durability. The usage of POE-g-MAH could contribute to the impressive balance between high rigidity and high toughness. However, the mass of the POE-g-MAH/CaCO₃/HDPE polymer composite should not be too high, and the proper mass range should be neither higher than 35% nor lower than 8%. Furthermore, trials and studies of the potential capacity and mechanical property of the HDPE-PPR-POE-g-MAH/CaCO₃/HDPE blended system were also performed. Results showed that the gaps between recycled and non-recycled materials would be further reduced with the help of the POE-g-MAH/CaCO₃ microcapsules, and such a blended system promises great commercial value in the industry.

AUTHOR INFORMATION

Corresponding Author

Yuanzhe Li – College of Polymer Science and Engineering, Sichuan University, Chengdu 610065, China; School of Chemistry and Biomolecules Engineering, National University of Singapore, 637551, Singapore; School of Materials Science & Engineering, Nanyang Technological University, 639798, Singapore; orcid.org/0000-0001-7530-8286; Email: yuanzhe001@e.ntu.edu.sg

Authors

Yutong Wang – College of Polymer Science and Engineering, Sichuan University, Chengdu 610065, China

Lichang Lu – College of Polymer Science and Engineering, Sichuan University, Chengdu 610065, China; School of Advanced Materials Science and Engineering, Loughborough University, Loughborough LE11 3TT, United Kingdom

Yu Hao – School of Chemistry and Biomolecules Engineering, National University of Singapore, 637551, Singapore

Yujie Wu – College of Polymer Science and Engineering, Sichuan University, Chengdu 610065, China; School of Chemistry and Biomolecules Engineering, National University of Singapore, 637551, Singapore

Complete contact information is available at:
<https://pubs.acs.org/10.1021/acsomega.1c02354>

Notes

The authors declare no competing financial interest.

ACKNOWLEDGMENTS

This research was funded by the MOE Academic Research Fund (AcRF) Tier 1 Project “Nano-structured Titania with tunable hydrophilic/hydrophobic behavior and photocatalytic function for marine structure application,” Grant Call (Call 1/2018) _MSE (EP Code EP5P, Project ID 122018-T1-001-077), Ministry of Education (MOE), Singapore, the National Natural Science Foundation of China (Grant number 51704258), and the Natural Science Foundation of Hunan Province, China (Grant No. 2019JJ50587).

■ REFERENCES

- (1) Long, N.; Hsuan, G. Y.; Spataro, S. Life Cycle Economic and Environmental Implications of Pristine High-Density Polyethylene and Alternative Materials in Drainage Pipe Applications. *J. Polym. Environ.* **2017**, *25*, 925–947.
- (2) Saur, K.; Fava, J. A.; Spataro, S. Life cycle engineering case study: automobile fender designs. *Environ. Prog.* **2000**, *19*, 72–82.
- (3) Lloyd, S. M.; Lave, L. B. Life cycle economic and environmental implications of using nanocomposites in automobiles. *Environ. Sci. Technol.* **2003**, *37*, 3458–3466.
- (4) Recio, J. B.; Baldasano, J. M.; Guerro, P. J.; Ageitos, M. G.; Narváez, R. P. Estimate of energy consumption and CO₂ associated with the Preproduction. *Use and Final Disposal of PVC, HDPE, PP. Ductile Iron and Concrete Pipes, Barcelona* (2005).
- (5) Juliane, P.-R.; Ferregueti, A. C.; Bergallo, H. G.; Rocha, C. F. D. Use of Polyvinyl Chloride Pipes (PVC) as Potential Artificial Shelters for Amphibians in a Coastal Plain Forest of Southeastern Brazil. *J. Coastal. Conserv.* **2017**, *21*, 327–331.
- (6) Majid, F.; Elghorba, M. Continuum Damage Modeling through Theoretical and Experimental Pressure Limit Formulas. *Frat. ed Integrita Strutt.*, *43* (), 79–89, DOI: 10.3221/IGF-ESIS.43.05.
- (7) Kim, J.-S.; Yoo, J.-H.; Oh, J.-Y. A Study on Residual Stress Mitigation of the HDPE Pipe for Various Annealing Conditions. *J. Mech. Sci. Technol.* **2015**, *29*, 1065–1073.
- (8) Latifa, A.; Azzouz, S.; Chaoui, K. Reliability Index of HDPE Pipe Based on Fracture Toughness. *Mechanika*, *23* (), 820–825.
- (9) Deng, C.; Jin, B.; Zhao, Z.; Shen, K.; Zhang, J. The Influence of Hoop Shear Field on the Structure and Performances of Glass Fiber Reinforced Three-layer Polypropylene Random Copolymer Pipe. *J. Appl. Polym. Sci.* **2019**, *136*, 46985.
- (10) Chen, J.; Wang, G.; Zeng, X.; Zhao, H.; Cao, D.; Yun, J.; Tan, C. K. Toughening of Polypropylene-Ethylene Copolymer with Nanosized CaCO₃ and Styrene-butadiene-styrene. *J. Appl. Polym. Sci.* **2004**, *94*, 796–802.
- (11) Ge, Q.; Wu, T.; Ding, L.; Yang, F.; Xiang, M. Effect of Annealing on Microstructure and Mechanical Properties of Polypropylene Random Copolymer. *Soft Mater.* **2019**, *17*, 1–13.
- (12) Hao, W.; Li, W.; Yang, W.; Shen, L. Effect of silicon nitride nanoparticles on crystallization behavior of PP. *Polym. Testing* **2011**, *30*, 527–533.
- (13) Hussain, F.; Hojjati, M.; Okamoto, M.; Gorga, R. E. Review article: polymer matrix nanocomposites, processing manufacturing and application an overview. *J. Compos. Mater.* **2006**, *40*, 1511–1575.
- (14) ASTM International ASTM D638-14, *Standard Test Method for Tensile Properties of Plastics*; ASTM International: West Conshohocken, PA, 2014, www.astm.org.
- (15) ASTM International ASTM D790-17, *Standard Test Methods for Flexural Properties of Unreinforced and Reinforced Plastics and Electrical Insulating Materials*; ASTM International: West Conshohocken, PA, 2017, www.astm.org.
- (16) Devi, S. H. K.; Shashidhara, G. M.; Ghosh, A. K. Characterization of HDPE/MMT-based nanocomposites. *Compos. Interfaces* **2010**, *17*, 217–222.
- (17) Deepthi, M. V.; Sharma, M.; Sailaja, R. R. N.; Anantha, P.; Sampathkumaran, P.; Seetharamu, S. Mechanical and thermal characteristics of high density polyethylene-flyash cenospheres composites. *J. Mater. Des.* **2010**, *31*, 2051–2060.
- (18) Sarker, M.; Rashid, M. M.; Molla, M. Abundant High-Density Polyethylene (HDPE-2) turns into fuel by using of HZSM-5 catalyst. *J. Fundam. Renew. Energy Appl.* **2013**, *1*, 1–12.
- (19) Ray, S. S.; Okamoto, M. Polymer/layered silicate nanocomposites a review from preparation to processing. *Prog. Polym. Sci.* **2003**, *28*, 1539–1641.
- (20) Wang, X.; Mi, J.; Wang, J.; Zhou, H.; Wang, X. Multiple actions of poly(ethylene octene) grafted with glycidyl methacrylate on the performance of poly(lactic acid). *RSC Adv.* **2018**, *8*, 34418–34427.
- (21) Zhon, W.; Wang, C.; Ai, T.; Wu, K.; Zhao, F.; Gu, H. A novel fibre reinforced polyethylene composite with added silicon nitride particles for enhanced thermal conductivity. *Composites, Part A* **2009**, *40*, 830–836.
- (22) Shi, G.; Zhang, M. Q.; Rong, M. Z.; Wetzel, B.; Friedrich, K. Friction and wear of low nanometer Si₃N₄ filler epoxy composites. *Wear* **2003**, *254*, 784–796.
- (23) Hussain, F.; Hojjati, M.; Okamoto, M.; Georga, R. E. Polymer-matrix nanocomposites, processing manufacturing and application an overview. *J. Compos. Mater.* **2006**, *40*, 1511–1575.
- (24) Croitoru, C.; Alexandru, P.; Roata, I. C.; Stanciu, E.-M. Obtaining and Characterization of Polyolefin-Filled Calcium Carbonate Composites Modified with Stearic Acid. *IOP Conf. Ser. Mater. Sci. Eng.* **2017**, *209*, No. 012041.
- (25) Deepthi, M. V.; Sailaja, R. R. N.; Sampathkumaran, P.; Vynatheya, S.; Seetharamu, S. Study of tribological properties of cenospheres filled HDPE composites. *Mater. Sci. Indian J.*, *6* (), 8–12.
- (26) Zhang, M. Q.; Rong, M. Z.; Zhang, H. B.; Friedrich, K. Mechanical Properties of Low Nano-silica Filled High Density Polyethylene Composites. *Polym. Eng. Sci.* **2003**, *43*, 490–500.
- (27) Xu, G. C.; Wang, J.; Ji, X. L.; Xiong, J. X.; Li, F. Effect of nanosilicon nitride on the mechanical electric properties of polypropylene nanocomposite. *J. Compos. Mater.* **2007**, *41*, 2213–2223.
- (28) Deka, B. K.; Maji, T. K. Effect of nanoclay and Zn O on the physical and chemical properties of wood polymer nanocomposite. *J. Appl. Polym. Sci.* **2012**, *124*, 2919–2929.